Available online at www.sciencedirect.com

SCIENCE DIRECT

Cement and Concrete Research 35 (2005) 2233–2243

Cement and Concrete Research

Solid state NMR and LVSEM studies on the hardening of latex modified tile mortar systems

J. Rottstegge[a,1], M. Arnold[a], L. Herschke[a], G. Glasser[a], M. Wilhelm[a], H.W. Spiess[a,*], W.D. Hergeth[b]

[a]*Max Planck Institute for Polymer Research, Ackermannweg 10, D-55128 Mainz, Germany*
[b]*Wacker Polymer Systems GmbH and Co. KG, Johannes Hess Straße 24, D-84483 Burghausen, Germany*

Received 29 March 2004; accepted 1 October 2004

Abstract

Construction mortars contain a broad variety of both inorganic and organic additives beside the cement powder. Here we present a study of tile mortar systems based on portland cement, quartz, methyl cellulose and different latex additives. As known, the methyl cellulose stabilizes the freshly prepared cement paste, the latex additive enhances final hydrophobicity, flexibility and adhesion. Measurements were performed by solid state nuclear magnetic resonance (NMR) and low voltage scanning electron microscopy (LVSEM) to probe the influence of the latex additives on the hydration, hardening and the final tile mortar properties. While solid state NMR enables monitoring of the bulk composition, scanning electron microscopy affords visualization of particles and textures with respect to their shape and the distribution of the different phases.

Within the alkaline cement paste, the poly(vinyl acetate) (VAc)-based latex dispersions stabilized by poly(vinyl alcohol) (PVA) were found to be relatively stable against hydrolysis. The influence of the combined organic additives methyl cellulose, poly(vinyl alcohol) and latexes stabilized by poly(vinyl alcohol) on the final silicate structure of the cement hydration products is small. But even small amounts of additives result in an increased ratio of ettringite to monosulfate within the final hydrated tile mortar as monitored by ^{27}Al NMR. The latex was found to be adsorbed to the inorganic surfaces, acting as glue to the inorganic components. For similar latex water interfaces built up by poly(vinyl alcohol), a variation in the latex polymer composition results in modified organic textures. In addition to the networks of the inorganic cement and of the latex, there is a weak network build up by thin polymer fibers, most probably originating from poly(vinyl alcohol). Besides the weak network, polymer fibers form well-ordered textures covering inorganic crystals such as portlandite.

Keywords: Mortar; Organic materials; Cement paste; Solid state NMR; LVSEM

1. Introduction

Commercial cements and mortars are quite complex systems. Portland cement as one of the ingredients consists of a variety of inorganic calcium aluminates and silicates [1–4]. Several components like calcium sulfate, alkali oxides, MgO and Fe_2O_3 within the portland cement modify the crystallization during the hydration and hardening [1–9]. When water is added to the cement powder, ettringite (trisulfate, $Ca_6Al_2O_6(SO_4)_3$*$32H_2O$ [1]) is formed. The high water content of ettringite results in an enormous increase of volume at the surface of the cement grains. When the cement paste runs poor in sulfate concentration, monosulfate ($Ca_4Al_2O_6SO_4$*$12H_2O$) is formed by consuming the trisulfate partially. Finally sulfate-free components can also be formed. In addition to this fast crystallization process, there is a slow reaction of the silicates within the calcium silicates and of the iron oxides, which form higher condensed aggregates during the hydration, resulting in a network of calcium aluminate hydrates and calcium silicate hydrates.

* Corresponding author. Tel.: +49 6131 379120; fax: +49 6131 379320.
E-mail address: spiess@mpip-mainz.mpg.de (H.W. Spiess).
[1] Current address: Institute of Chemistry, The Chinese Academy of Sciences, 100080 Beijing, PR China.

0008-8846/$ - see front matter © 2004 Elsevier Ltd. All rights reserved.
doi:10.1016/j.cemconres.2004.10.003

Cement is commonly modified by inorganic compounds such as quartz or gravel and fillers. Inorganic and organic additives can be summarized with respect to their influence on the setting and hardening of cement [5–8]. Concrete plasticizers and super plasticizers are the most common organic cement additives, other additives retard setting or hardening or accelerate it. Stabilizers bind water and adjust viscosity, thereby stabilizing the freshly prepared cement paste. Air entraining agents enable pores in the final hardened cement paste. Waterproofing agents commonly consist of fatty acids or latex dispersions and afford hydrophobicity in the hardened paste by means of filling the pores and sealing the final hydrated cement. Here, questions concerning size and surface of the latex particles as well as their ability to form films arise. Additionally, the polymer latex acts as organic binder and promotes improved adhesion and flexibility to the hardened cement paste [10].

In addition to the influence of the additives on the mechanical properties during cement hardening as described above, the molecular interactions can modify the final crystal structure and growth, even in small amounts of organic additives [11–15]. This effect is caused by either adsorbing onto the growing inorganic surfaces or by binding aqueous ions into a complex or a salt. Such adsorbed organic components modify ionic diffusion near the inorganic substrate and can alter specific crystal growth.

The objective of our study is to elucidate the influence of various latex additives on the hydration/hardening and on the final texture of portland cement-based tile mortars by combining spectroscopic and microscopic techniques [16–19]. Solid state NMR spectroscopy [20–23] monitors the bulk composition and its changes during the hydration process of both the hardened cement and the polymers. Thus, differences in the tile mortar systems with respect to the bulk composition can be determined. Low voltage scanning electron microscopy (LVSEM) [24–27] enables visualization of the particle shapes of the hydrated cement phases and the latex. Electron microscopy detects the differences within the tile mortar systems with respect to the shape of their microscopic morphology. Several contributions to the hydration and hardening of cement pastes as determined from ^{1}H, ^{27}Al and ^{29}Si NMR [28–38] and scanning electron microscopy methods [39–41] are available in the literature. The presented work extend these methodologies into a combined NMR and LVSEM study of latex modified tile mortar systems to monitor the influence of the organic components on the hydration and hardening of the cement paste at a microscopic level. While ^{27}Al NMR monitors the hydration reaction products of the calcium aluminate clinker phases [1–9], ^{29}Si NMR is sensitive to the slow silicate condensation during the hydration. Specifically the ^{27}Al NMR signals can be correlated with defined crystal structures within the inorganic phase [29,30]. The individual shape of the different phases within the hardened cement texture can be obtained by scanning electron microscopy. Here multiple hydrated cement phases can be correlated with structures known from the literature [39–42].

2. Materials and methods

2.1. Materials

The tile mortar systems presented here contain about 25–50 wt.% of portland cement, quartz, 0.1–0.5 wt.% cellulose ethers and 3–20 wt.% of latex. In principle latex dispersions can be applied to the cement as aqueous dispersion or as dispersion powder [16–19]. In this study, dispersions were applied as redispersible powders made from dispersions stabilized by poly(vinyl alcohol). Latex polymers were chosen to be poly(vinyl acetate co-ethylene), poly(vinyl acetate co-ethylene co-versatic acid vinyl ester) and poly-(vinyl chloride co-ethylene co-vinyl laurate) copolymers. Poly(vinyl alcohol) was used as surfactant during emulsion polymerization and was subsequently added in combination with anti-blocking agents (e.g. minerals) to ensure the latex powder redispersibility. The latex powder contained about 15 wt.% of poly(vinyl alcohol) and 10 wt.% of the anti-blocking agents in addition to the latex particle polymers. The final tile mortar product would contain additional wetting agents and defoamers.

Several tile mortar samples were prepared from Rohrdorfer cement CEM I 42.5R, fine milled quartz, methyl cellulose and various polymer latex dispersion powders as summarized in Table 1. Already the applied portland cement “Rohrdorfer Zement CEM I 42.5 R” is a mixture of various oxides,

Table 1
Composition of the tile mortar samples in %

Sample	Cement	Quartz	Dispersion powder	P(VA co-VAc) in dispersion powder	MC, P(AAm co-AA)	Water
Tm1	42.3	54.3	3.0	0.15	0.4, –	83.3
Tm2	80.2	–	19.1	0.95	0.4, –	83.3
Tm3	42.3	54.3	3.0	0.3	0.4, 0.05	83.3
Tm4	42.3	54.3	3.0	0.26	0.4, –	83.3
Tm5	42.3	54.3	3.0	0.18	0.4, –	83.3
Tm6	80.2	–	19.1	1.15	0.8, –	83.3
Tm7	42.3	54.3	3.0	0.3	0.4, –	83.3

As cement the Rohrdorfer cement CEM I 42.5R was taken. Samples were adjusted to a constant water/cement ratio. The abbreviations P(VA co-VAc), MC and P(AAm co-AA) are poly(vinyl alcohol co-vinyl acetate), methyl cellulose and poly(acrylamide co-acrylic acid); respectively. Poly(vinyl alcohol co-vinyl acetate) is part of each dispersion powder. The amount of water is given in wt.% based on dry matter (100 wt.%).

aluminates and silicates with the elemental composition described elsewhere [42]. Walocel® MKX 40000 PF 01 from Wolff Walsrode was applied as methyl cellulose. All latex powder samples contain poly(vinyl alcohol) at a degree of 88 mol.% hydrolysis as stabilizer originating from emulsion polymerization and further added to the dispersion as a poly(vinyl alcohol)/anti-blocking agent (minerals) admixture for the spray drying of the dispersion. Latex polymers were poly(vinyl acetate co-ethylene), poly(vinyl acetate co-ethylene co-versatic acid vinyl ester) and poly(vinyl chloride co-ethylene co-vinyl laurate) copolymers as summarized in Table 2. Tile mortar 3 additionally contains low amounts of a thickener made from poly(acrylamide co-acrylic acid). The glass transition temperatures (T_g) of all latexes were found to be below the room temperature, the minimum film formation temperatures (MFT) as determined on a temperature gradient bar [43] were found to be close to the freezing point of water for all the samples. Particle sizes of the latex particles were determined by a Malvern Instruments Zetasizer 3000 HS. The particle sizes were determined to be about 1 μm in diameter for both the investigated dispersions and the redispersed powders. Due to the applied emulsion polymerization performed under semi-batch conditions up to 20% smaller particles of 200- to 300-nm size were additionally found. Particles of the dispersed anti-blocking agents were determined to a size of about 3 to 10 μm.

2.2. Sample preparation

Tile mortar powder samples (composition in Table 1) were carefully mixed for 10 min to achieve a sufficient homogeneity and stored in closed PE flasks. The hydrated and hardened cement paste was obtained from these samples by adding distilled water to the samples, applying a constant water/cement ratio, while stirring them carefully for several minutes. The compositions of the hydrated tile mortar systems Tm1 to Tm7 are summarized in Table 1. Preparation, hydration and hardening were again performed in closed PE flasks to prevent water evaporation from the samples, carbonization by CO_2 from the air [44], or alkali contamination from glass. For these hydration and hardening experiments, samples were stored at room temperature for a variable time. A complete water uptake was found for most samples within one day. A decelerated water uptake was found for tile mortar 4 and 5. Even after four days of hardening, not all water was consumed, while tile mortar 7 contained even excessive dispersion at this time. After specific hardening times, samples were milled and investigated by different solid state NMR methods and by LVSEM.

Table 2
Characterization of investigated latex polymer systems

Tile mortar	Dispersion polymer	T_g (°C)	MFT (°C)
Tm1, Tm2	P(VAc-E)-1	−7	0
Tm3	P(VAc-E)-1	−7	0
Tm4	P(VAc-E-VeoVa)	−14	0
Tm5, Tm6	P(VAc-E)-2	16	4
Tm7	P(VC-E-Vinyl laurate)	1	0

VAc: vinyl acetate, E: ethylene, VeoVa: vinyl ester of versatic acid 10, VC: vinyl chloride, MFT: minimum film formation temperature.

2.3. Solid state NMR

Nuclear magnetic resonance (NMR) spectroscopy [20–23,45] can be applied for both liquids and solids. In solids, broadening interactions of nuclear spins are no longer averaged, consequently, the solid state NMR spectra are characteristically broadened. In principle, the line width in amorphous solid materials is related to the chemical environment and the local mobility within the investigated sample. The line width of ^{1}H, ^{13}C, ^{27}Al and ^{29}Si spectra in solid state NMR can be reduced by spinning the sample at the magic angle (magic angle spinning, MAS) [23] where typical rotation frequencies are currently in the range of 2–35 kHz.

The ^{13}C, ^{27}Al and ^{29}Si NMR spectra were acquired using Bruker DSX 300 and DSX 500 spectrometers, operating at magnetic fields of 7.05 and 11.74 T. All ^{13}C CP MAS spectra [23] were measured using 4-mm rotors with a commercial double-resonance probehead and spinning speeds of 8 kHz at temperatures of 233 an 243 K. ^{27}Al NMR measurements were performed with 4-mm probes, ^{29}Si NMR with a 7-mm probe. The CP time within the ^{13}C CP MAS experiments was 2 ms at a ^{1}H 90° pulse length of 4 μs and at a recycle delay 2 s. For ^{27}Al NMR measurements, the 90° pulse length was 4 μs at a recycle delay time of 5 s, while 5 μs as 90° pulse length and 60 s as recycle delay were applied for ^{29}Si NMR measurements.

2.4. Low voltage scanning electron microscopy

The low voltage scanning electron microscopy (LVSEM) images were taken from dry chunks and powders of the freshly split concrete samples with a LEO Gemini 1530 SEM without sample sputtering. Samples were fixed to the substrate by means of conductive adhesive tapes or carbon glue. The accelerating voltage of the applied field emission gun was between 1 and 3 kV. Applying an aperture size of 20 or 30 μm, the working distance was between 3 and 6 mm, generally around 5 mm.

3. Results and discussion

3.1. Principles of latex modified concrete

Our investigations are focused on the influence of various latex additives on the hydration/hardening and on the final texture of portland cement-based tile mortars. The pH within the aqueous cement paste was about 13, so the stability, specifically the aging of the latex modified tile mortar system is an important issue. Due to the high pH,

there is a probability of hydrolysis/saponification of organic additives like poly(vinyl acetate) copolymers to poly(vinyl alcohol). The decomposition of pure PVAc dispersions within the hardened cement paste is well known [46]. Upon decomposition, the poly(vinyl acetate) forms $Ca(CH_3CO_2)_2$ and poly(vinyl alcohol). In order to clarify the latex stability within the alkaline medium, NMR measurements were performed on the polymer composition prior and after the hydration and hardening. Only minor differences in the ^{13}C-CP MAS spectra of tile mortar 2 were detected at an increased P(VAc-E)-1 content before and after 14 days of hydration as can be seen from the spectra in Fig. 1a. Additionally, no $Ca(CH_3COO)_2$ ^{13}C NMR signals could be recorded. So the latex P(VAc-E) core at about 22 wt.% ethylene is stable with respect to hydrolysis. These data are in good agreement with the previous mechanical measurements, showing no decrease in flexural and compressive strength of hardened cement pastes within 10 years [47]. For comparison, the ^{13}C CP MAS spectra of both the initial latex powder additive and of tile mortar 6 after 30 days of hydration and hardening are shown in Fig. 1b. ^{13}C CP MAS spectra are clearly different for the latex polymer P(VAc-E)-2 in tile mortar 6 at the reduced ethylene content of about 9 wt.%. After hardening, the signal ratios of the CHO and CH_2 groups to the CO and CH_3 groups have changed indicating a polymer decomposition due to partial hydrolysis. The additional line broadening of the CHO and CH_2 signals observed in the spectra is due to changes in the resonance frequencies of poly(vinyl acetate) and of poly (vinyl alcohol). Resonance frequency changes from 40 to 45 ppm for the CH_2 signal and from 67 to 70 ppm for the CHO signal directly reflect hydrolysis. The latex is therefore stable against hydrolysis at 22 wt.% ethylene, but shows partial hydrolysis for ethylene contents of 9 wt.% or less.

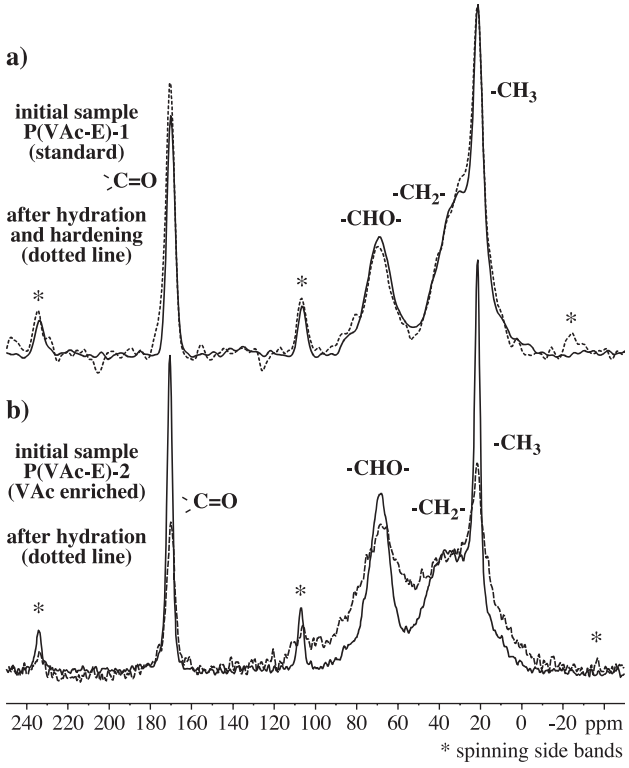

Fig. 1. ^{13}C CP MAS spectra before and after hydration and hardening (a) of tile mortar 2 measured at a temperature of 233 K and (b) of tile mortar 6 measured at a temperature of 243 K and at a MAS frequency of 8 kHz.

During emulsion polymerization of vinyl acetate (VAc), the growing polymer chains are known to react partially with the stabilizer poly(vinyl alcohol) (PVA) and to form PVA-graft-PVAc copolymers [48,49]. The amount of the grafted, water insoluble PVA was found to exceed 20% of the total 30 wt.% PVA applied for the stabilization [48]. Consequently, the resistance against hydrolysis of PVA stabilized PVAc latex particles is increased due to the grafted protecting colloid.

In the LVSEM image of Fig. 2a, the latex is found to be adsorbed to the inorganic surfaces and to cover them. Due to the low latex concentration of 3 wt.%, no complete film formation is observed. Even in the best case scenario, just a partial latex film formation can be expected. Latex film formation requires a close contact of latex particles. Film formation might therefore succeed latex adsorption and latex coagulation. But the latex is competing with the PVA and the methyl cellulose for the adsorption onto the inorganic surfaces. As a result, the hydrated cement surfaces are covered by both, PVA stabilized latex particles and excessive PVA. Latex particles or films can be found among the inorganic components, sticking them together as a glue under appropriate conditions. This can be seen in the scanning electron micrograph of tile mortar 1 in Fig. 2b. Here the latex is sticking between the portlandite crystals. Nevertheless, the space between the hydrated cement grains is filled by ettringite needles as shown in Fig. 2c.

Polymer (additive) cement interactions can alter the inorganic structures and products during hydration. The cement pastes, used in this study, contain methyl cellulose, poly(vinyl alcohol) and latexes stabilized by poly(vinyl alcohol). Therefore, the influence on the crystal growth and the hydration of the organic additives is expected to be similar to that of the individual stabilizing additives methyl cellulose and poly(vinyl alcohol) [42]. By adding the sum of the organic additives to the cement paste, a reduced monosulfate/ettringite ratio is obtained as shown by ^{27}Al NMR in Fig. 3. This ratio is even more reduced upon an addition of the pure methyl cellulose. The influence of the latex, PVA and the methyl cellulose on the ^{29}Si NMR spectra is weak.

Principles on the role of the latex within the hardened cement paste are already described in the literature [50]: The latex particles reduce the viscosity of the cement paste. The particles can be used to replace water in the cement paste and to modify the process window of the paste or to change the setting time. During the hydration and hardening, the latex particles cover the inorganic surfaces and form an additional organic network. Microcracks due to the material shrinking might therefore be covered by latex

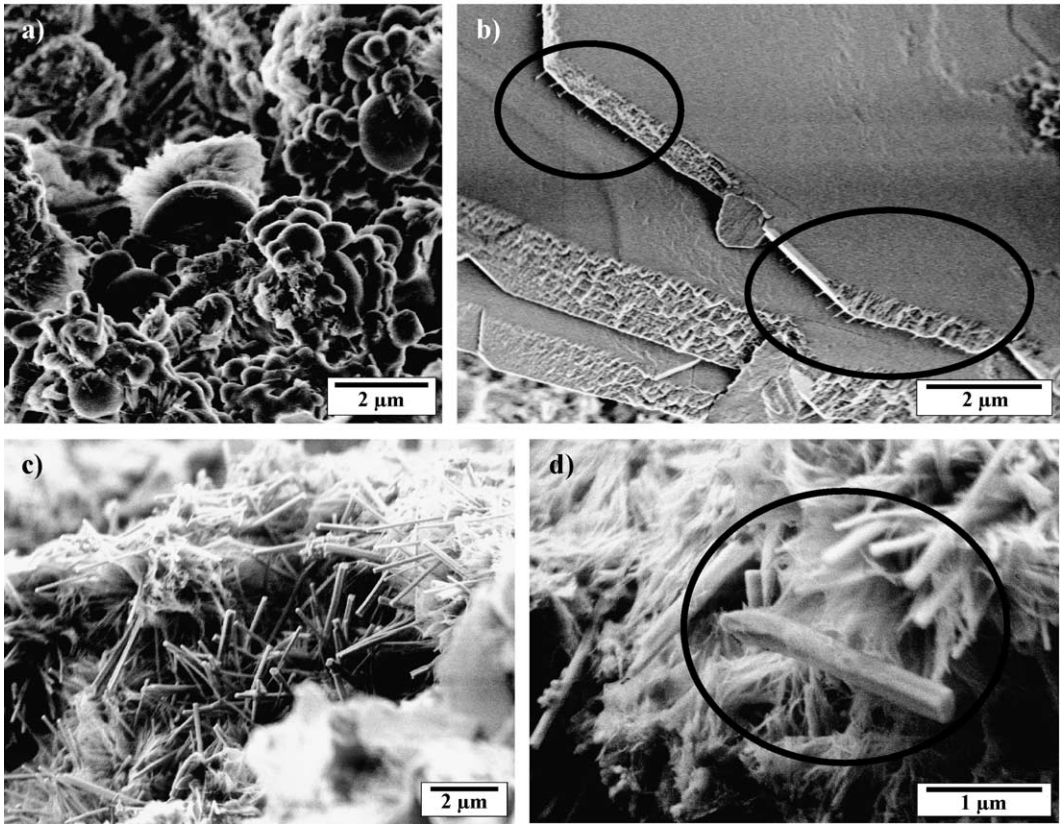

Fig. 2. LVSEM micrographs of the hardened cement pastes after two month of hydration: (a) tile mortar 5 showing the latex being adsorbed to the inorganic surfaces, (b) tile mortar 1 imaging latex particles sticking and stretched between portlandite crystals, (c) tile mortar 5 showing ettringite needles filling the space between the cement grains, (d) an ettringite needle fixed to the hardened cement paste by latex within tile mortar 4.

within the hardened cement paste, their propagation might be terminated or retarded [50]. Additionally, the latex provides an improved adhesion to surfaces and the pore filling seals the material.

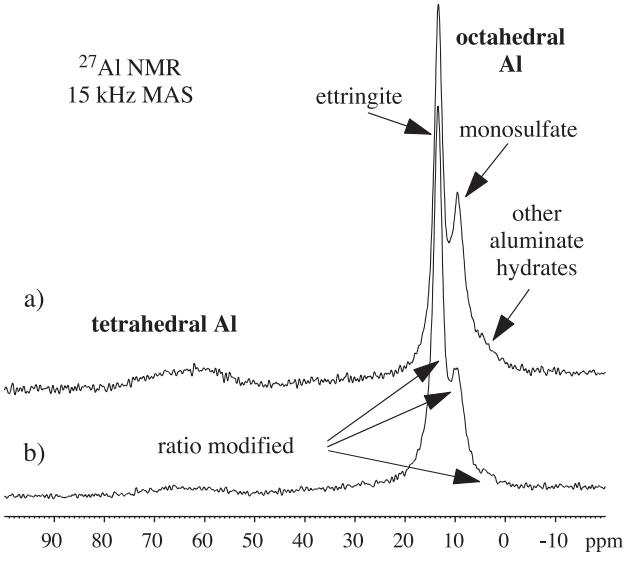

Fig. 3. ^{27}Al solid state NMR spectra of hardened cement pastes (a) without and (b) with latex and poly(vinyl alcohol co-vinyl acetate) in tile mortar 1 after 10 months of hydration and hardening measured at 15 kHz MAS.

3.2. Differences due to latex composition

Differences in latex systems are due to variations in the surfactant layer, which result in changes in the polymer water interface [51], in the latex polymer and in the particle morphology. Within the present study, changes in the final properties of latex modified hardened cement pastes result from latexes having similar interfaces built up by P(VA-co-VAc) but different latex core polymers. The latex polymers applied in this work differ in their hydrophilicity and T_g. While T_g influences the film formation, hydrophilicity alter diffusion of water and ions as well as hydration and crystallization. Here only small differences in T_g are present with a maximum deviation of 30 °C. All latex systems form films at room temperature according to their minimum film formation temperature (MFT) of 0 or 4 °C. Polarity varies from quite polar and hydrophilic, e.g. poly(vinyl acetate) copolymers to hydrophobic, e.g. vinyl chloride ethylene-based polymers.

Latex particles or films in close proximity to portlandite were generally taken for the detailed LVSEM analysis: In principle it is possible to find latex particles (by LVSEM) close to a wide variety of inorganic crystals, the CSH and CAH phases and both aluminum and silicate-free components. Electron micrographs of latex particles close to portlandite crystals (Fig. 2b) or to an ettringite needle (Fig. 2d) are shown as examples. Large and brittle crystals

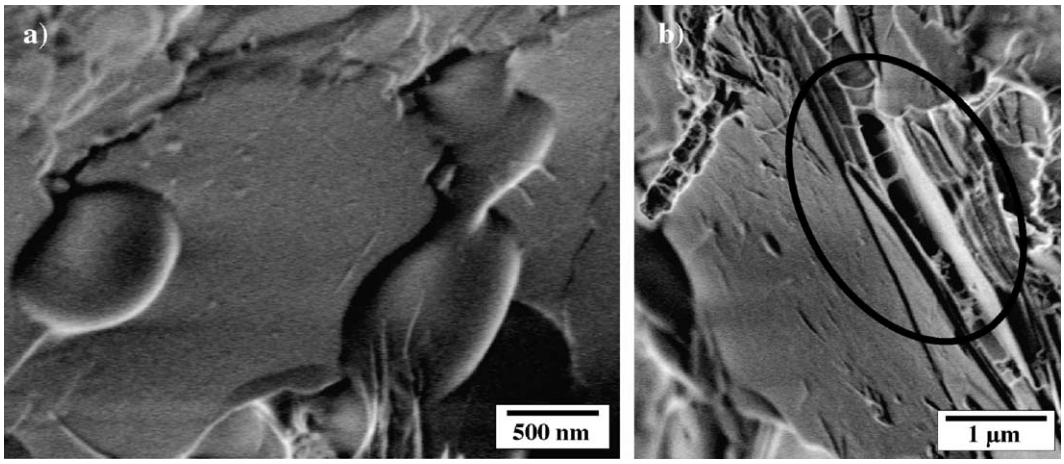

Fig. 4. SEM images of tile mortar 3 after hydration and hardening with the latex particles (a) sticking to and (b) between portlandite crystals.

like ettringite and portlandite are most relevant from a mechanical point of view. Additionally, due to the crystal shape of portlandite ($Ca(OH)_2$), microcracks caused by shear are easily visible within the hardened cement texture. The variations in latex modified tile mortar systems, presented in this study, therefore, describe differences in the latex shape close to portlandite (by LVSEM) and in the composition of the inorganic texture as detected by NMR.

Within the LVSEM images of Fig. 4, the latex of tile mortar 3 (compare with Fig. 2b on tile mortar 1) is found be to adsorbed onto the calcium hydroxide surfaces. The latex nestles to the crystal surface, indicating a high compatibility of both. A gap between the different portlandite plates is visible, connected by latex filaments. Similar latex filaments close to portlandite crystals can be found within the electron micrographs of tile mortar 4 in Fig. 5 after the hydration and hardening. The shape of the latex, especially of the latex filaments connecting the gap—visible in details in Fig. 5b and also in Fig. 2d—is different. Latex lamellae and filaments possess a rather high surface roughness. Lamellae and surfaces are not fully relaxed to a minimum surface area. The latex within tile mortar 4 was optimized for improved adhesion properties.

In contrast to this, the original particle shape of the "high T_g" latex with particle sizes ranging from 200 nm to 1 µm within tile mortar 5 is still visible as shown in Fig. 6. Here a portlandite crystal is shown, bound by latex particles to the hardened cement matrix. Only partial film formation can be observed even after 1 month of hydration and hardening. By manual cracking, the final tile mortar is found to be more brittle. In Fig. 7, the hydrophobic poly(vinyl chloride co-ethylene) latex within tile mortar 7 is found to be partially aggregated. The latex is sticking close to the inorganic crystals and shows better film formation than the polar "high T_g" latex. In contrast to the good compatibility between the latex and the portlandite surface in tile mortar

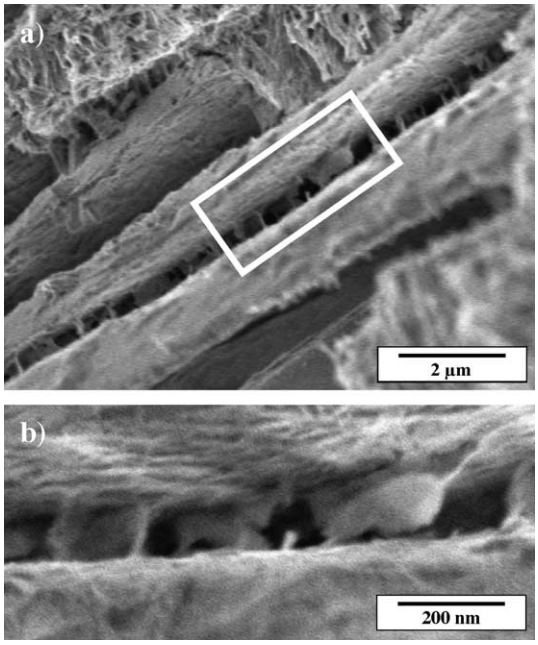

Fig. 5. Electron micrographs of tile mortar 4 after hydration and hardening showing the latex sticking between portlandite crystals given (a) as an overview and (b) as a detailed view.

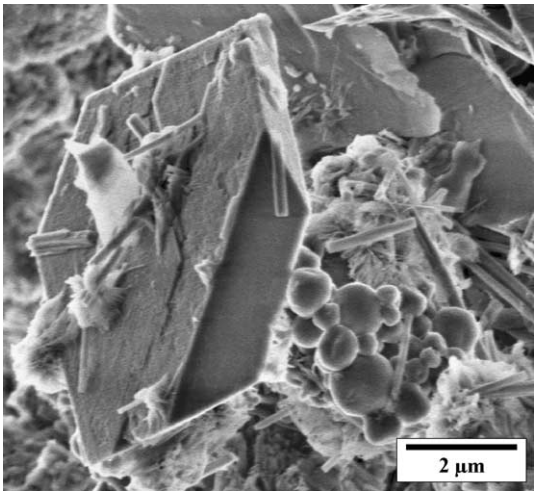

Fig. 6. Partially filmed latex within tile mortar 5. The latex sticks the portlandite to the hardened cement matrix.

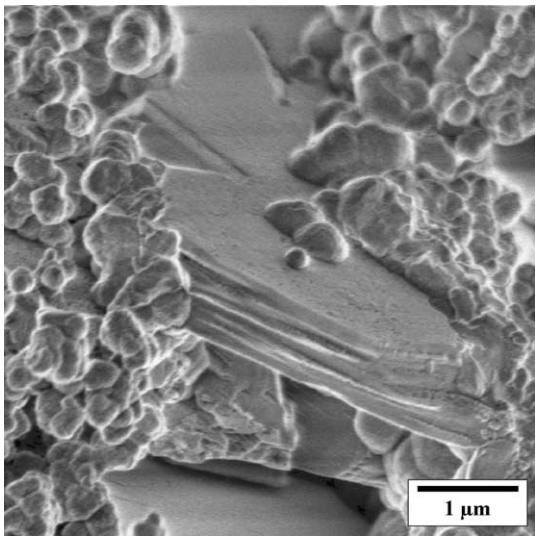

Fig. 7. Partially filmed latex within tile mortar 7 between the inorganic crystals after hydration.

1 and 3 (Fig. 4), the contact angle of the latex to the inorganic surface is clearly changed in tile mortar 7 as seen in Fig. 7. The reduced compatibility between the latex and the cement was already visible during sample preparation (Section 2.1). Although similar polymer water interfaces built up by poly(vinyl alcohol) are used in all latex systems, changes in the latex mortar compatibility are clearly visible. As shown in a previous study [47], the hydrophobic latex acts as a hydrophobizing agent. Once hardened, the water absorption was shown to be dramatically reduced.

3.3. Differences of inorganic composition

The change of the latex polymer also influences the composition of the inorganic texture. When water is added to the portland cement, hydration and crystallization take place. During hardening, the water is immobilized and bound to the inorganic matrix. Aluminum oxides and aluminates within the portland cement are converted from tetrahedral to octahedral co-ordination during hydration. In the ^{27}Al NMR spectra, tetrahedral co-ordination corresponds to a chemical shift of 80–90 ppm, while the octahedral resonances appear at 0–20 ppm. Within the ^{27}Al NMR spectra of hydrated cement [29,30], the signal at 13.2 ppm corresponds to ettringite, the resonance at 9.8 ppm corresponds to monosulfate ($Ca_4Al_2O_6SO_4$*$12H_2O$), while other aluminate hydrates can be detected at 5 ppm [30]. Calcium aluminosilicates contribute to both the weak ^{27}Al signal at 60–80 ppm [30,33] and at −5 to 10 ppm.

The condensation of the silicate components can be monitored by ^{29}Si NMR spectra. Original portland cement contains Q^0 groups in the initial CS phases (calcium silicate). There are no Si–O–Si bonds within the silicates; the silicates are isolated from each other. During hydration to CSH phases (calcium silicate hydrates), additional Q^1 and Q^2 groups are formed, as the silicates undergo condensation [31,32]. While Q^1 groups represent terminal end groups within the silicate network, Q^2 groups reflect silicate chains. Quartz (Q^4 groups), which is used as an inorganic filler, is integrated into the network during hydration and reorganization of the portland cement.

In a previous study, the portland cement quartz mixture was, along with other additives, modified with methyl cellulose and poly(vinyl alcohol co-vinyl acetate) [42]. Both are commonly applied as stabilizers to bind water to the freshly prepared cement paste [6]. During hydration and hardening, both organic additives were immobilized and adsorbed to the inorganic matrix. In addition to the stabilizing effect, the additives modify the Al distribution between ettringite, monosulfate and other aluminate hydrates. It was found that more ettringite is formed if low amounts of 0.4 wt.% methyl cellulose or poly(vinyl alcohol co-vinyl acetate) at 88% hydrolysis are applied. The silicates within the hydrated cement show a higher degree of condensation without cellulose ethers, while the influence of poly(vinyl alcohol) on the silicate condensation is weak as detected by ^{29}Si NMR [42]. Poly(acrylic acid) and poly(-acrylamide) as additives have a strong influence on the mechanical properties of a freshly prepared cement paste acting as thickening/stabilizing agents, however their effect on the NMR spectra of the final hardened cement is weak. The stabilizing effect is enhanced compared to adsorption and modification of crystal growth especially for high molecular weight additives [42].

As seen in the ^{27}Al NMR spectra of Fig. 8, the ratio of the hydration products ettringite to monosulfate changes

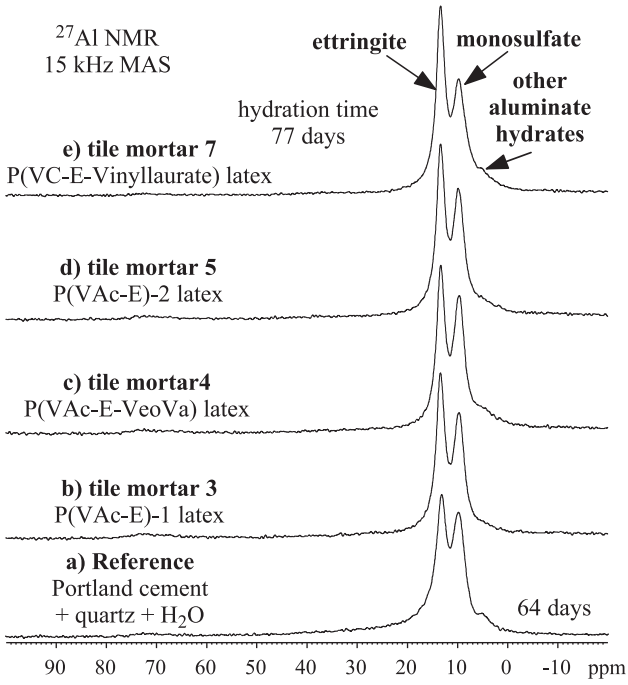

Fig. 8. ^{27}Al solid state NMR spectra of hardened cement pastes without (a) and with latex and poly(vinyl alcohol co-vinyl acetate) in tile mortar 3 to 7 (b–e) after 2 month of hydration and hardening measured at 15 kHz MAS.

depending on the applied latex polymer. The ettringite/monosulfate ratio is increased in a similar way for all vinyl acetate-based latex polymers within tile mortar 3 to 5. The ettringite formation is even more dominant for the hydrophobic vinyl chloride-based latex within tile mortar 7. In contrast to the ^{27}Al NMR spectra, the influence of the combined organic additives on the ^{29}Si NMR spectra is weak and will not be discussed here.

Weak effects of the latex T_g on the final properties of the hardened cement pastes are reported in the literature at small amounts of the latex additive [47,52,53]. Increasing T_g was found to increase compressive strength and to reduce shear and adhesion strength of the tile mortar. These findings nicely complement our results on the compatibility of the latexes with the hydrated cement matrix.

3.4. Fibril structures and networks

In addition to the inorganic texture modified by the latex, well-ordered fibers can be found within the hardened cement admixture as shown in Fig. 9a. Beside the "high T_g" latex particles of tile mortar 5 adsorbed to the hydrated cement, additional fibers are visible covering a portlandite crystal. As presented in Fig. 9b, these fibers are oriented in three directions according to the crystal axes of portlandite. With increased thickness, a more or less complete film can be found. Despite all changes in the chemical composition, these fibers could be detected within all investigated latex modified tile mortar systems but not in latex and poly(vinyl alcohol)-free samples (Fig. 9d). The ordering of the fibers according to the crystal axes of the portlandite can be best observed at low surface coverage as shown in Fig. 9c. At the right upper corner of the SEM image, the contrast is lost due to the fact that the portlandite is not oriented perpendicular to the camera, but at an angle of about 40°. For a vertical camera position, the angle between the fibers is found to be about 60°, which is in good agreement with the hexagonal structure of portlandite.

No thin fibers were found close to portlandite crystals within latex and poly(vinyl alcohol)-free hardened cement paste samples. In Fig. 9d, a LVSEM image of portlandite is shown without the fibers. Here the cement was hardened without latex and poly(vinyl alcohol) additives. The cement to methyl cellulose, quartz and water ratio was the same as within tile mortar 1 (see Table 1). Due to the composition of the organic admixture within the tile mortar samples

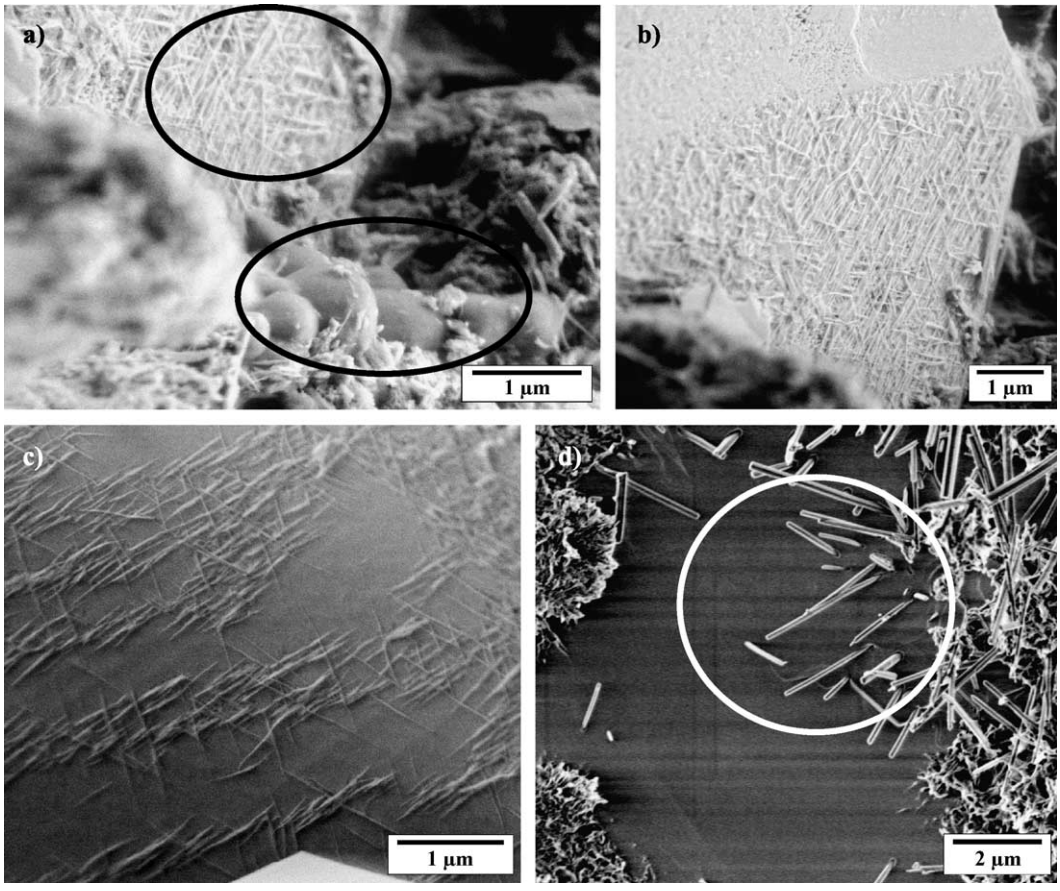

Fig. 9. LVSEM images of hardened cement pastes showing (a) partially filmed latex within tile mortar 5 (in front) and fibers (left upper corner), (b) ordered fibers within tile mortar 5 on portlandite along the crystallographic axis, (c) the hexagonal organization of the fibers on portlandite within tile mortar 7 at a camera tilt angle of about 40° to the portlandite crystal surface, (d) ettringite and gypsum needles piercing a fiber-free portlandite crystal within a latex and poly(vinyl alcohol)-free mortar sample.

consisting of hydrolysis resistant latex particles stabilized by poly(vinyl alcohol), excessive poly(vinyl alcohol) and low amounts of cellulose ethers, these fibers most probably consist of poly(vinyl alcohol). This is in accordance with the literature, reporting on a fiber formation during saponification of poly(vinyl esters) [54] and on a worm-like texture of a poly(vinyl alcohol) hydrogel as prepared by freeze etching of a 8 wt.% PVA solution in water [55] as detected by LVSEM.

The fiber layer changes structure during electron beam exposure. A series of images was taken during exposure at a vertical camera position as presented in Fig. 10. While Fig. 10a depicts the initial situation close to the beginning of the exposure (after 10 s), the exposure time (dose) is increasing via Fig. 10b taken at 100 s to the applied maximum as shown in Fig. 10c at 200 s. The irradiation of substrates with an electron beam results in a charging and heating of the exposed structures. While many inorganic structures are quite resistant to low exposure doses at a acceleration voltage of 1 to 3 kV, most organic components melt, are cleaved or finally removed at high exposure doses. As seen in Fig. 10a–c, the e-beam exposure of the fiber textures results in both melting and material removal. The melting of the structures causes the formation of a dense film, while in the center of the electron beam close to the highest exposure dose, the material is removed.

Similar polymer fibers can also be found forming a network within the hardened cement paste. In Fig. 11, a finespun web from polymer fibers filling the space between ettringite needles is shown after hydration and hardening of tile mortar 5. Here no macroscopic orientation within the network can be found. Again the fiber structures can easily be removed by the e-beam exposure and are not found in poly(vinyl alcohol)-free samples. For most polymers, an aggregation of a dissolved polymer to bulk material would generally be expected upon drying. Here the fibers as depicted in Fig. 11 are elongated to a length of a few hundred nanometers. The web formed from the polymeric fibers might be correlated with the original morphology of the PVA within the aqueous solution between the cement grains [55]. Additionally, it should be kept in mind that the

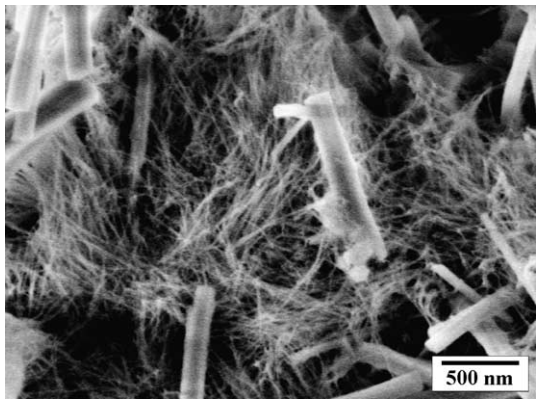

Fig. 11. Network from polymer fibers in tile mortar 5 beside the larger ettringite needles after hydration.

poly(vinyl alcohol co-vinyl acetate) forms fibers at a high degree of hydrolysis.

So polymer fibers form both, well-ordered layers on inorganic crystals like portlandite and weak networks between the crystals. The polymer fiber structures are present in addition to the organic network of the latex. As a result, both the latex and the polymer fibers can be observed within the electron micrographs in Fig. 12a and b sticking between portlandite crystals within tile mortar 7. In addition to the well-known latex network, the combined organic network provides enforced mechanical flexibility to the hardened cement paste.

4. Conclusion

Solid state NMR and scanning electron microscopy methods were used to determine the composition and texture of tile mortar systems and the influence of organic additives on the hydration and hardening of cement pastes. The investigated tile mortar systems were made from portland cement, quartz, methyl cellulose and redispersible latex powders. All dispersion powders were stabilized by poly (vinyl alcohol co-vinyl acetate) at 88% hydrolysis. Latex polymers were chosen to be poly(vinyl acetate co-ethylene),

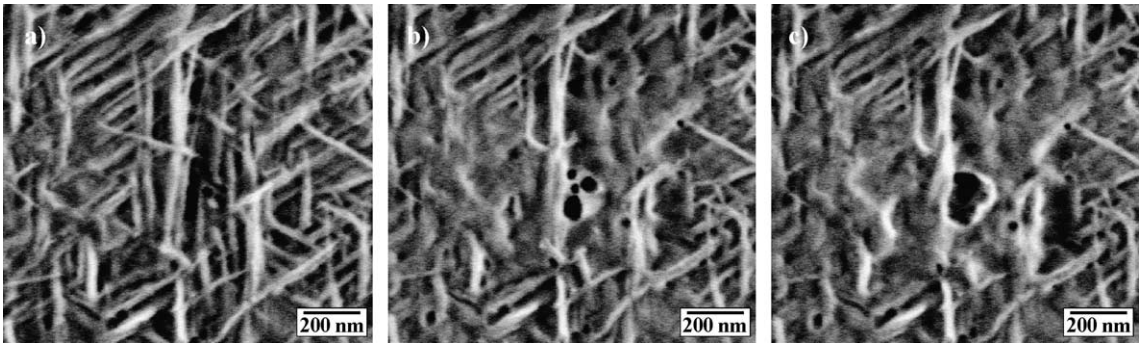

Fig. 10. Film formation of polymer fibers and polymer removal during e-beam exposure in tile mortar 7 (left to right: increasing exposure time of about (a) 10, (b) 100 and (c) 200 s).

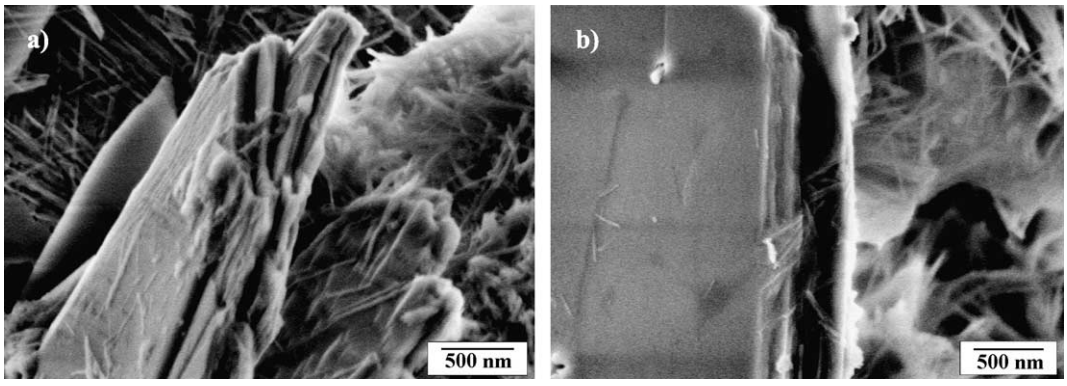

Fig. 12. Latex and polymer fibers sticking between portlandite in tile mortar 7 after hydration.

poly(vinyl acetate co-ethylene co-versatic acid vinyl ester) and poly(vinyl chloride co-ethylene co-vinyl laurate) copolymers. As the pH within the cement paste is about 13, especially the stability of the vinyl acetate copolymers against hydrolysis is an important issue. Only minor differences can be found within the ^{13}C CP MAS spectra of the corresponding tile mortars before and after hydration and hardening at an ethylene comonomer content of 22 wt.% within the poly(vinyl acetate co-ethylene) latex polymer. The spectra clearly change at 9 wt.% comonomer content. So latexes from vinyl acetate ethylene copolymers stabilized by PVA are found to be stable against the alkaline medium at an ethylene content of about 22 wt.%, while partial hydrolysis occurs for ethylene contents of 9 wt.% or lower.

The latex within the tile mortar system is adsorbed to the inorganic surfaces and acts as glue for the crystals. Latex particles are known to provide increased flexibility to the concrete, which can be traced down to the microscopic length scale. Due to the low concentration of 3 wt.%, partial latex film formation only is observed. Addition of PVA stabilized latexes and methyl cellulose changes the distribution of aluminum to the crystallization products as detected by ^{27}Al NMR. Hardening in the presence of the added PVA stabilized latexes results in an increased ettringite monosulfate ratio within the hydrated cement, while the influence of the organic additives on the silicate hydration and condensation is weak.

Despite the small differences in T_g of 30 °C and in hydrophilicity between the quite polar and hydrophilic poly(vinyl acetate) copolymers and the hydrophobic vinyl chloride ethylene-based polymers marked differences in the latex modified tile mortar systems are found. Taking latexes close to portlandite ($Ca(OH)_2$) as sensors for LVSEM analysis, the vinyl acetate-based latexes generally show a small contact angle and therefore a good compatibility with the calcium hydroxide surface. At a T_g below 0 °C, the latex sticks well to and between the portlandite crystals and acts as a glue. At a T_g of 16 °C, a reduced latex particle coalescence and adhesion to the portlandite is found. The compatibility between the latex and the portlandite is clearly reduced for the hydrophobic poly(vinyl chloride co-ethylene)-based latexes. This results in an increase in the contact angle between both phases. A change in the latex polymer additionally modifies the hydration products of the aluminate clinker phases. While only minor differences in the silicate structure can be found between the various vinyl acetate-based latex polymers, the ettringite/monosulfate ratio is clearly increased for the vinyl chloride-based latex.

The inorganic texture is modified by latexes and thin fibers within all tile mortar systems but not in latex and poly(vinyl alcohol)-free samples. Due to the fact that the investigated latex additives have different latex polymers but similar surfactant interfaces made from poly(vinyl alcohol), the fibers are most probably polymers deriving from excessive, not grafted PVA. These polymer fibers order on portlandite crystal surfaces according to the crystal axes having an angle of 60° between the three main directions. Beside these ordered structures, the polymer fibers form an organic network in addition to the latex network. On low dose e-beam exposure, these fibers form films, while at high doses the fibers are finally removed.

Acknowledgement

We would like to acknowledge the helpful discussions with J. Grinshtein, R. Graf (Max Planck Institute), I. Alig, H. Oehler (Deutsches Kunststoff Institut), U. Komm (Mamorit) and last, but not least the funding by the BMBF (grant No. 01RC0177).

References

[1] H.F.W. Taylor, Cement Chemistry, 2nd edition, Telford Publishing, London, 1997.
[2] J. Benstedt, P. Barnes, Structure and Performance of Cements, Spon Press, London, 2002.
[3] M.B. Bever, Encyclopedia of Materials Science and Engineering, 1st ed., vol. 1, Pergamon Press, Oxford, 1986, p. 566f.
[4] H. Ost, B. Rassow, Lehrbuch der chemischen Technologie, 26th edition, Johann Ambrosius Barth Verlag, Leibzig, 1955, p. 429.
[5] e.V. Deutsche Bauchemie, Modified Mineral Mortar Systems and the Environment, 1998, www.deutsche-bauchemie.de.
[6] e.V. Deutsche Bauchemie, Concrete Admixtures and the Environment, 1999, www.deutsche-bauchemie.de.

[7] U.S. Department of Transportation, Federal Highway administration, Set-Acceleration, 1999, www.fhwa.dot.gov.
[8] U.S. Department of Transportation, Federal Highway administration, Set-Retarding, 1999, www.fhwa.dot.gov.
[9] J.F. Young, A review of the mechanism of set-retardation in portland cement pastes containing organic admixtures, Cem. Concr. Res. 2 (1972) 415–443.
[10] J. Schulze, Thermoplastische Polymere—Modifikation von Mörteln und Beton, Beton 5 (1991) 232–237.
[11] W.A. Tiller, The Science of Crystallization: Microscopic Interfacial Phenomena, 1st edition, Cambridge University Press, Cambridge, 1991.
[12] J.M. Marentette, J. Norwig, E. Stockelmann, W.H. Meyer, G. Wegner, Crystallization of $CaCO_3$ in the presence of PEO-block-PMMA copolymers, Adv. Mater. 9 (1997) 647–665.
[13] S. Mann, Biomineralization: Chemical and Biochemical Properties, 1st edition, Wiley, Weinheim, 1989.
[14] E. Baeuerlein, Biomineralization: From Biology to Biotechnology and Medical Application, 1st edition, Wiley, Weinheim, 2000.
[15] G. Wegner, P. Baum, M. Mullert, J. Norwig, K. Landfester, Polymers designed to control nucleation and growth of inorganic crystals from aqueous media, Macromol. Symp. 175 (2001) 349–355.
[16] R.P. Bright, Comparison of liquid dispersions with spray-dried acrylic polymers as mortars of cement-based patching material, Cem., Concr. Aggreg. 17 (1995) 227–230.
[17] X.H. Ci, R.R. Falconio, Acrylic powder modified portland cement, Cem., Concr. Aggreg. 17 (1995) 218–226.
[18] J. Schulze, Tonind.-Ztg. 109 (1985) 689–697.
[19] H. Lutz, C. Hahner, in: D. Urban, K. Takamura (Eds.), Polymer Dispersions and their Industrial Applications, 1st edition, Wiley, Weinheim, 2002.
[20] P. Colombet, A.R. Grimmer, H. Zanni, P. Sozzani, Nuclear Magnetic Resonance Spectroscopy Of Cement-Based Materials, Springer, Berlin, 1998.
[21] P. Colombet, A.R. Grimmer, Application of NMR Spectroscopy to Cement Science, Gordon and Breach Science Publishers, 1994.
[22] G. Engelhardt, D. Michel, High-Resolution Solid-State NMR of Silicates and Zeolites, John Wiley & Sons, Chichester, 1987.
[23] K. Schmidt-Rohr, H.W. Spiess, Multidimensional Solid-State NMR and Polymers, Academic Press, London, 1994.
[24] P. Buseck, J. Cowley, L. Eyring, High-Resolution Transmission Electron Microscopy and Associated Techniques, Oxford University Press, New York, 1992.
[25] L. Reimer, Scanning electron microscopy: physics of image formation and microanalysis, in: W.T. Rhodes (Ed.), Springer Series in Optical Sciences, vol. 45, Springer, Berlin, 1988.
[26] J.H. Butler, D.C. Joy, G.F. Bradley, S.J. Krause, Low voltage scanning electron-microscopy of polymers, Polymer 36 (1995) 1781–1790.
[27] D.L. Vezie, E.L. Thomas, W.W. Adams, Low-voltage, high resolution scanning electron-microscopy—a new characterization technique for polymer morphology, Polymer 36 (1995) 1761–1779.
[28] G.E. Maciel, Silica surfaces: characterization, in: D.M. Grant, R.K. Harris (Eds.), Encyclopedia of Nuclear Magnetic Resonance, vol. 7, John Wiley & Sons, Chichester, 1996, pp. 4370–4386.
[29] J. Skibsted, E. Henderson, H.J. Jakobsen, Characterization of calcium aluminate phases in cements by ^{27}Al MAS NMR spectroscopy, Inorg. Chem. 32 (1993) 1013–1027.
[30] M.D. Andersen, H.J. Jakobsen, J. Skibsted, Incorporation of aluminum in the calcium silicate hydrate (C–S–H) of hydrated portland cements: a high-field ^{27}Al and ^{29}Si MAS NMR investigation, Inorg. Chem. 42 (2003) 2280–2287.
[31] P. Faucon, T. Charpentier, D. Bertrandie, A. Nonat, J. Virlet, J.C. Petit, Characterization of calcium aluminate hydrates and related hydrates of cement pastes by ^{27}Al MQ-MAS NMR, Inorg. Chem. 37 (1998) 3727–3733.
[32] P. Faucon, J.C. Petit, T. Charpentier, J.F. Jacquinot, F. Adenot, Silicon substitution for aluminum in calcium silicate hydrates, J. Am. Ceram. Soc. 82 (1999) 1307–1312.
[33] G. Engelhardt, M. Nofz, K. Forkel, F.G. Wihsmann, M. Mägi, A. Samoson, E. Lippmaa, Phys. Chem. Glasses 26 (1985) 157–165.
[34] E. Lippmaa, M. Mägi, A. Samoson, G. Engelhardt, A.R. Grimmer, Structural studies of silicates by solid-state high-resolution ^{29}Si NMR, J. Am. Chem. Soc. 102 (1980) 4889–4893.
[35] D. Müller, A. Rettel, W. Gessner, G. Scheler, An application of solid-state magic-angle-spinning ^{27}Al NMR to the study of cement hydration, J. Magn. Res. 57 (1984) 152–156.
[36] E. Lippmaa, M. Mägi, M. Tarmak, W. Wieker, A.R. Grimmer, A high resolution ^{29}Si NMR study of the hydration of tricalciumsilicate, Cem. Concr. Res. 12 (1982) 597–602.
[37] J.R. Barnes, A.D.H. Clague, N.J. Clayden, C.M. Dobson, C.J. Hayes, G.W. Groves, S.A. Rodger, Hydration of portland cement followed by ^{29}Si solid-state NMR spectroscopy, J. Mater. Sci. Lett. 4 (1985) 1293–1295.
[38] J. Roncero, S. Valls, R. Gettu, Study of the influence of superplasticizers on the hydration of cement paste using nuclear magnetic resonance and X-ray diffraction techniques, Cem. Concr. Res. 32 (2002) 103–108.
[39] D. Barthelmy, Mineralogy Database, 2002, www.webmineral.com.
[40] J. Stark, B. Möser, A. Eckart, 14. Internationale Baustofftagung-ibausil, Weimar, 20–23.09.2000, Volume 1, pp. 1093–1109, 2000.
[41] U. Nürnberger, Korrosion und Korrosionsschutz im Bauwesen, Bauverlag, Wiesbaden, 1995.
[42] J. Rottstegge, M. Wilhelm, H. W. Spiess, Solid state NMR investigations on the role of additives on the hydration and hardening of cement pastes, submitted to Cement and Concrete Research.
[43] T.F. Protzman, G.L. Brown, An apparatus for the determination of the minimum film temperature of polymer emulsions, J. Appl. Polym. Sci. 4 (1960) 81–85.
[44] J. Aguilera, M.T. Blanco-Varela, S. Martinez-Ramirez, Thermodynamic modeling of the $CaO–SiO_2–CaCO_3–H_2O$ closed and open system at 25° C, Mater. Constr. 53 (2003) 35–43.
[45] R.R. Ernst, G. Bodenhausen, A. Wokaun, Principles of Nuclear Magnetic Resonance in One and Two Dimensions, Clarendon Press, Oxford, 1986.
[46] H. Lutz, in: D. Distler (Ed.), Wäßrige Polymerdispersionen, Wiley, Weinheim, 1999, p. 230.
[47] J. Schulze, O. Killermann, Long-term performance of redispersible powders in mortars, Cem. Concr. Res. 31 (2001) 357–362.
[48] G.S. Magallanes Gonzalez, V.L. Dimonie, E.D. Sudol, H.J. Yue, A. Klein, M.S. El-Aasser, Characterization of poly(vinyl alcohol) during the emulsion polymerization of vinyl acetate using poly(vinyl alcohol) as emulsifier, J. Polym. Sci., A 34 (1996) 849–862.
[49] I. Gavat, V. Dimonie, D. Donescu, C. Hagiopol, M. Munteanu, K. Gosa, T. Deleanu, Grafting process in vinyl acetate polymerization in the presence of nonionic emulsifiers, J. Polym. Sci., C Polym. Symp. 64 (1978) 125–140.
[50] J.E. Isenburg, J.W. Vanderhoff, Hypothesis for reinforcement of portland cement by polymer latexes, J. Am. Ceram. Soc. 57 (1974) 242.
[51] K. Yuki, T. Murakami, H. Narukawa, T. Okaya, Fluidity and mechanical properties of cement mortars containing poly(ethylene-co-vinyl acetate) emulsions, Nippon Kagaku Kaishi (1994) 571–576.
[52] F.P. Petrocelli, C.F. Cordeiro, Continuous process for the production of vinyl acetate-ethylene emulsion copolymers, Macromol. Symp. 155 (2000) 39–51.
[53] L.A. Kuhlmann, Properties of a non-film forming latex in ceramic tile mortar, Cem., Concr. Aggreg. 17 (1995) 208–217.
[54] W.S. Lyoo, W.S. Ha, In situ fibrillation of poly(vinyl alcohol) during saponification of poly(vinyl ester) (I). Chemorheological and morphological investigations of in situ fibrillation, Polymer 40 (1999) 497–505.
[55] H. Trieu, S. Qutubuddin, Poly(vinyl alcohol) hydrogels: 2. Effect of processing parameters on structure and properties, Polymer 36 (1995) 2531–2539.